Available online at www.sciencedirect.com

ScienceDirect

Procedia Environmental Sciences 38 (2017) 331 – 339

Procedia Environmental Sciences

International Conference on Sustainable Synergies from Buildings to the Urban Scale, SBE16

Monitoring and Simulation of Diurnal Surface Conditions of a Wooden Façade

Thomas K. Thiis [a,*], Ingunn Burud[a], Andreas Fløa, Dimitrios Kraniotis[b] Stergiani Charisi[a], Petter Stefansson[a]

[a]*Department of Mathematical Science and Technology, Norwegian University of Life Sciences, Box 5003, 1432, ÅS, Norway*
[b]*Norwegian Institute of Wood Technology, Forskningsveien 3b, 0314 OSLO, Norway*

Abstract

The hygrothermal surface conditions of a façade is important for the degradation of the façade material as well as for the energy budget of the building. The distribution of short term variations of the temperature and moisture in the façade is often neglected in degradation studies that will typically treat the whole façade equally. The moisture and temperature variations are especially important in porous building materials where water dependent biological and physical processes are the main degrading factors.

In this study the diurnal cycle of the surface temperature is measured with conventional temperature probes as well as with infra-red camera. In addition, the moisture content of the wooden façade is measured with resistive measurement technique.

The measurements are used to validate simulations of the spatial temperature and moisture variations on the façade. The study shows large variations of surface conditions on the façade and that the simulations reproduces the measurements within a high degree of accuracy.

Peer-review under responsibility of the organizing committee of SBE16.

Keywords: Façade; buildings; climate; simulations; measurements; IR

1. Introduction

The surface climate of facades is important for the service life of the cladding. Porous building materials will interact with moisture and temperature, creating internal stresses as the temperature varies as well as creating

* Corresponding author.
E-mail address: thomas.thiis@nmbu.no

Peer-review under responsibility of the organizing committee of SBE16.
doi:10.1016/j.proenv.2017.03.088

conditions for biological activity such as mould and algae. New developments in architecture are moving towards less surface treatment, and more use of untreated wooden surfaces as cladding. Untreated wood is naturally colored by climatic exposure. The colouring of wooden surfaces is often a result of mould growth and lignin deterioration. Humidity, temperature and exposure time of these are the main drivers of mould growth on a specific material.

The surface conditions of the wooden cladding can be simulated by Heat and Moisture (HAM) simulations, taking into account indoor and outdoor climate as well as the physical properties of the wall. However, for well-insulated buildings, the effect of the interior climate on the outdoor surface conditions is small and sometimes negligible. The temperature and moisture conditions on an exterior wall will have a large variability. A windowsill protruding only a few centimetres from the wall will create a zone on the wall, which is shaded from solar radiation and driving rain. On such facades, the variation of the exterior microclimate might be more important for the deterioration than the heat and moisture transport through the wall.

This paper describes two simple models for surface temperature and moisture on a wooden façade. The models are driven by exterior climate data, which is combined with ray-tracing to account for the micro scale variations of the solar irradiance on the wall. The models are validated with measurements from an untreated wooden façade, which shows uneven colouring and stains, which are clearly caused by uneven climatic exposure of the façade.

2. Simulation model

2.1 Surface temperature.

The one-dimensional Fourier's law, $q_x = -k\frac{dT}{dx}$, describes the heat flux in a material. Here q_x [W/m^2] is the heat flux in the x-direction, k is the thermal conductivity and T is temperature. In numerical simulations of fluid and mass transfer, it is often necessary to know the wall surface temperature. This is commonly found by applying a special case of Fourier's law called the Heat Flux Boundary Conditions in which the surface temperature of a body is determined by:

$$T_w = \frac{q_{room}+q_{stored}-q_{rad}}{h} + T_a \quad (1)$$

Here T_w is the wall surface temperature, q_{room} is the heat flux from the interior trough the wall, q_{rad} is the radiative heat flux from the surroundings, q_{stored} is the heat flux caused by heating or cooling the material in the wall, h is the local heat transfer coefficient and T_a is the temperature of the fluid near the surface. In the example shown later in the paper, the effect of convection within wall cavities is excluded. In situations with little or no radiation from the surroundings, i.e. when the sun is down, q_{room} can be found by:

$$q_{room} = \frac{dT_{wall}}{R_{wall}} \quad (2)$$

Where R_{wall} [m^{2}K/W] is the thermal resistance of the wall. In a common, modern building q_{room} is in the order of 3 to 10 W/m^2 in a cold climate. Since the solar irradiance often will be in the range of several hundred W/m^2, q_{room} will be negligible during hours when the sun is over the horizon. The heat flux from stored thermal energy in the building material, q_{stored} can be found using:

$$q_{stored} = \frac{cmdT_{t\_wall}}{at} \quad (3)$$

where c [J/kgK] is the specific heat capacity, m [kg] is the mass of the wall material contributing and dT_{t_wall} [K] is the temperature change of the material over a specific time t [s] and a [m^2] is the unit area of the wall.

This means that q_{stored} is 0 as long as there is no change in temperature of the wall material. The solar radiation, q_{rad} is usually measured on meteorological stations, and will in cases with no cloud cover be possible to estimate based on solar position and standard atmospheric conditions. On meteorological stations, it is usually the direct radiation on a horizontal surface together with the diffuse radiation that is measured. The direct solar radiation on a facade can be found knowing the inclination and direction of the façade as well as the solar position, and transforming the direct radiation using trigonometry. It is important to note that the radiative heat flux on a surface should be corrected for the reflected amount of the radiation. q_{rad} is therefore $q_{rad}=\alpha q_{solar}$ where α is the absorption coefficient of the surface material.

The geometry of a building is also important when determining the radiation on the cladding. The solar radiation distribution on a wall is subject to local shading which will change with the position of the sun during the course of

the day. Accurate information about the solar radiation on the façade at every point in time and space is therefore necessary to simulate the surface temperature and thus the growth conditions of mould on the surface.

The model for surface temperature outlined above needs input of the solar radiation on the façade in time and space to run. The software tool RADIANCE has been developed to simulate the radiation in illuminated spaces. It uses the technique of ray-tracing, which follows light backwards from the image plane to the source. RADIANCE and another daylight simulation engine, DAYSIM (3), has been incorporated in the software DIVA-for Rhino, which provides a user friendly input to the simulation engine. The software has been used to calculate the climate-specific hourly irradiation at nodes located on the façade of a 3D digital building model. The software uses the well-known .epw (EnergyPlusWeather) files that provide hourly weather data for more than 2000 locations in the world.

Using a relatively dense simulation grid with one node every 8x8 cm gives the possibility to simulate the shading effects of small features like window-sills protruding from the façade as well as the larger effects as shading roof eave and inside corners. The software calculates the hourly solar radiation in every node for one whole year given the climate and the geographic position of the building.

2.2 Surface moisture and relative humidity (RH)

The relation between temperature, water content and RH is important in meteorological forecasting and is studied by several authors. The Clausius–Clapeyron equation characterizes the phase transition of water as temperature and pressure changes. The August-Roche-Magnus approximation gives a good approximation of this equation and Bolton (4) gives a set of coefficients for the approximation where RH is found from:

$$RH = 100\frac{\exp(\frac{aT_d}{b+T_d})}{\exp(\frac{aT}{b+T})} \tag{4}$$

here T is the air temperature, a=17.67, b=243.5 and T_d is the dew point temperature given by

$$T_d = \frac{b[\ln(\frac{RH}{100})+\frac{aT}{b+T}]}{a-\ln(\frac{RH}{100})-\frac{aT}{b+T}} \tag{5}$$

Assuming that the air in the boundary layer has the same absolute water content as the ambient air and that the temperature on the surface of a building is varying with the parameters given in the previous section, the RH in the boundary layer can be found by combining equations (5) and (4), substituting ambient air temperature T_a for T in eq. (5) and substituting T_w for T in eq. (4). I.e. the dew point T_d is calculated for the ambient air and RH is calculated using the dew point and the modelled surface temperature from equation (1).

The relation between RH in the air and equilibrium moisture content (EMC) in porous materials is usually determined with a mixture of laboratory test of diffusion and capillary moisture transport. He et al. (5) provides the moisture storage function for aspen based on the modified Oswin model. The free saturation and maximum water content is set to 600 and 700 kgm^{-3} respectively. Some façade materials are porous and can store water in its pores. However, most mould growth models use the relative humidity in the air and not the moisture in the material as argument. In a controlled climate with little variation in a laboratory, this is a good estimate, but in a natural environment where the variation is larger, this will no longer be valid. Wood will reach its equilibrium moisture content (EMC) after a given time in air with a specific RH. The time it needs to reach EMC is dependent on RH, temperature and wood substrate. Mazzanti and Uzielli (6) reports that an unpainted poplar wood panel subjected to a change in RH from 85 to 42% at a temperature of 30 degrees, loses 26% of the total desorbed water within the first hour. This is of course dependent on the surface to volume ratio of the sample, but indicates that the moisture content in wood is very sensitive to the sudden variations in environmental exposure. Modelling of moisture content in wood can be performed with models of different complexity and is a popular research topic. Several researchers has contributed to the field the last decades. One simple, empiric model for model dynamic for drying of biological material is the Page's model, eq .6 Here the moisture content in the material, *MC,* is expressed by the initial moisture content MC_i, the equilibrium moisture content *EMC*, time, *t*, the drying rate, *k* [h^{-1}] and the constant *n*. *k* and *n* are both dependent of the drying conditions i.e. temperature and air velocity.

$$MC = \exp(-kt^n)(MC_i - EMC) + EMC \tag{6}$$

He et al. (5) provides empirical data of temperature dependent *k* and *n* for aspen. However, in this study, only the

drying rate at 20 degrees [°C] is applied. At this temperature the drying rate is measured by He et al. (5) to be 0.016 [h^{-1}].

2.3. Wind driven rain

The moisture content of a cladding is also effected by driving rain. There has been several studies of the physics of driving rain, involving advanced Computational Fluid dynamics tools (7). However, the ISO standard ISO 15927-3:2009 given in Eq. 7 provides a straight forward calculation procedure and reasonably accurate results.

$$R_{wdr} = \frac{2}{9} C_R C_T O W U_{10} R_h^{0.88} \cos(\theta) \tag{7}$$

here R_h is the rainfall intensity [mm/h] C_T is the topography factor taking into account local wind speed up over hills and escarpments, C_R is the roughness factor which can be calculated to be 0,7 for a single detached house lower than 8 meters situated in a suburban area, θ is the angle between the wind direction and the surface normal and O is the obstruction factor which takes into account the effect of the closest neighboring objects. W is the wall factor, defined as the ratio of the quantity of water hitting the wall to the quantity passing through an equivalent unobstructed space. W is given for a limited number of façade configurations in the ISO standard, and for a two-story building with a flat roof it is defined to be ranging from 0.5 on the upper part of the façade to 0.3 on the lower part of the façade. The ISO model does not take into account micro scale effects of the wall. This might be the protrusion of a windowsill or the partial shielding of smaller scale geometry of the building. Numerical simulations of wind flow around buildings using Computational Fluid Dynamics has this capability, but only at a relatively high computational cost.

One simplified way to calculate the effect of small scale details on a wall is to use ray tracing. This will emulate the particle paths as straight lines, but a range of different azimuth and impact angles can be simulated for a large number of points at a low computational cost. The method has been in use to determine the solar radiation on surfaces for long time and is here used to determine the wall factor W in the ISO (10) model. The areas that are located in the rain shadow on the façade are determined for 16 different wind directions and 2 wind speeds with the

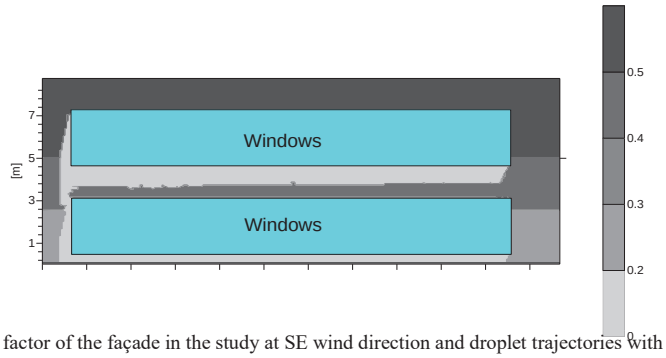

Fig. 1. Wall factor of the façade in the study at SE wind direction and droplet trajectories with a 65^0 angle.

use of the ray-tracing method. The 32 different masks are combined with the general wall factor creating a building specific wall factor. One example of the wall factor for the façade which is investigated in this study is shown in Figure 1. This wall factor is valid for South Eastern (SE) wind direction and rain droplet trajectories with a 65^0 angle. In this study the droplet trajectory angle is set to 65^0 when the wind velocity is < 4 m/s and 45^0 when the wind velocity is > 4 m/s.

Some of the driving rain hitting a façade will be absorbed and some will run off. These phenomena were reviewed by Blocken (8) who cite Beijer (9) simple model for this absorption *G(t)* in which

$$G(t) = min\begin{cases} available\ water \\ A\sqrt{t} \end{cases} \tag{8}$$

were A [$mm^3/mm^2\ s^{0.5}$]is the capillary water absorption coefficient set to 0.007. In the simulations, the absorbed

water is divided in the whole panel, which is 30 mm thick.

3. Measurements and simulations of diurnal temperature variation on an untreated wooden façade

The above models were applied to an untreated wooden façade made of 30 mm aspen panels. Behind the cladding, there is a layer of stagnant air. The façade is shown in Figure 2. The models were run with a hourly time step for a period of 12 months with meteorological input from a measurement station situated 1 km to the West of the building. The temperature and moisture in the panels was measured for a period of 3 months during the summer of 2015 and two weeks in the winter of 2016 to validate the model.

3.1 Measurements

The temperature sensors were installed in a hole drilled from the side of the panels 3 mm behind the surface. The moisture sensors were of the resistive type and the spikes were installed on the front side of the panels to be able to measure the occurrence of free water on the surface originating from driving rain. The position of the sensors are indicated in Figure 2. The sensors were logged every 30 minutes and the MC readings from the sensors were

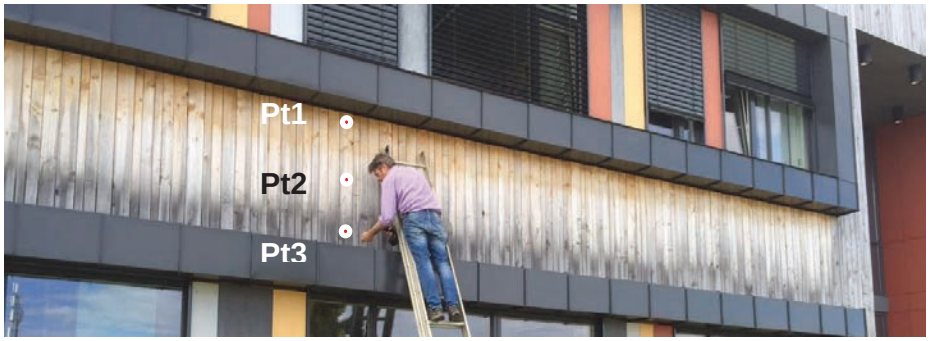

Fig. 2. Installation and position of sensors on untreated wooden façade.

temperature-corrected according to (11). The resistance based wood moisture measurements are affected by several factors, making the uncertainty of the measurements relatively large. However, in this study the sensors were installed in the same wood panel with less than 1 meter spacing, and the relative differences in the measurements are supposedly low enough to compare the different measurements.

In addition to the temperature sensors, infra red (IR) thermography was used to obtain the spatial distribution of surface temperature of the wooden façade of the building. An IR camera (Optris PI640) was mounted on the rooftop of the neighbouring building, monitoring the investigated façade for a time period of one week. Since the field of view of the camera was limited, the camera was set to two different directions. The camera was monitoring the right side of the south facing façade for 72 consecutive hours and the left side of the same façade for the next 84 hours. The IR camera was recording raw data in degrees Celsius with a time interval of 15 minutes.

The temperature sensor data are considered to be valid and reliable and they were used to validate the accuracy of the temperature data obtained by the IR camera. The whole monitoring period of the building façade lasted approximately a week. The camera was placed on a building roof across the examined building.

The emissivity of the wood used for the surface cladding of the building was unknown before the measurements. During the thermal camera recording, the emissivity of the surface material was set to 1 and later corrected based on the temperature measurements from the embedded sensors. Based on the calculated radiation power, the emissivity of the aspen was calculated to be ε=0.87. The raw surface temperatures obtained by the IR camera were corrected for emissivity of the material and the accuracy of the results was validated by the in-situ sensor data.

3.2 Simulations

The simulation is run with an hourly time step for 8770 hours in each of the approximately 22.000 nodes. The

input parameters to the proposed model for surface temperature are ambient air temperature, ambient RH, solar radiation, rain, wall R-value, surface transfer coefficients and indoor temperature which is set to 20^0 C. Wind direction and wind speed are used to determine which driving rain wall factor to use for each hourly time step. The hourly results that correspond to the monitoring days and area monitored by the IR camera, were extracted and are shown in the results section.

For the validation of the model, the surface temperatures predicted were compared with the corresponding surface temperatures acquired by the infrared camera for all the grid nodes and during the whole period of time. The root mean square error (RMSE) is used as a measure of the model performance. The RMSE of the simulation results is calculated by equation 9

$$RMSE = \sqrt{\frac{1}{n}\sum_{i=1}^{n} \Delta T^2} \quad (9)$$

where n is the overall time steps during which the surface temperatures were calculated and ΔT is the temperature difference between the measurements and the simulation model at each time step. The RMSE has previously been used to consider the accuracy of predicted model surface temperatures (12,13).

4. Results and Discussion

Figure 3 shows the measured and simulated diurnal variation of temperature on the three points monitored by sensors for a 72 hour period during winter and summer. The minimum and maximum temperatures during the summer conditions were 15 C^0 and 48 C^0 and on a partly cloudy day. During the winter, the amplitude of the temperature was larger, ranging from -12 C^0 to 48 C^0. The reason for the larger amplitude during winter, when the air temperature is lower than in summer, is probably due to the low solar angle. A low solar angle during winter will give more direct solar radiation on the façade than a higher angle during summer. The errors of the simulated

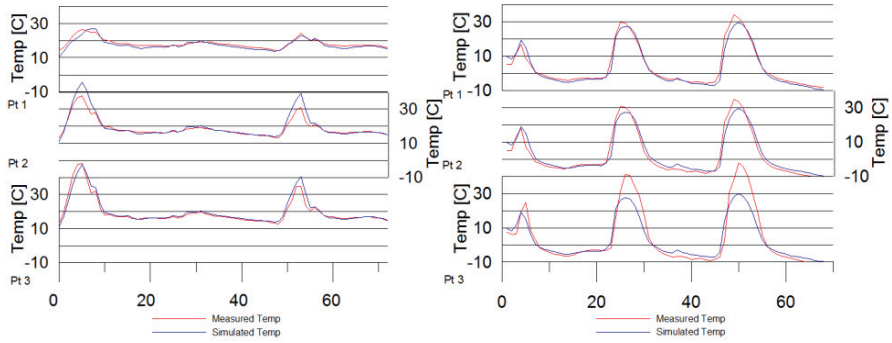

Fig. 3. Measured and simulated temperature in a 72 hour period during a) summer and b) winter.

temperatures compared to the measurements in the two periods are given in Table 1. The error is larges during winter time at the lowest point. This point is close to the window sill which is covered in a dark brown metal sheeting. The model does not include neither the metal sheeting nor the convective heat transfer from the windows sill, which presumably is quite large. The error might be caused by this simplification of the setup. Given the amplitude of the temperature, and compared to Yang et.al (12) the error of the simulations in the points is very low for such simple model.

Table 1. Root Mean Square Error (RMSE) of the simulation compared to the measurements in three points

	RMSE Pt1 [C^0]	RMSE Pt2 [C^0]	RMSE Pt3 [C^0]
Summer	1.23	2.46	1.87
Winter	2.21	2.79	6.03

Figure 4 shows the spatial distribution of the RMSE of the simulations compared to the IR measurements during two 72 hour episodes in winter. The two episodes were close in time, but episode B, shown on the right side of the façade in the figure, had lower ambient temperature. Even if the IR measurements were calibrate using surface

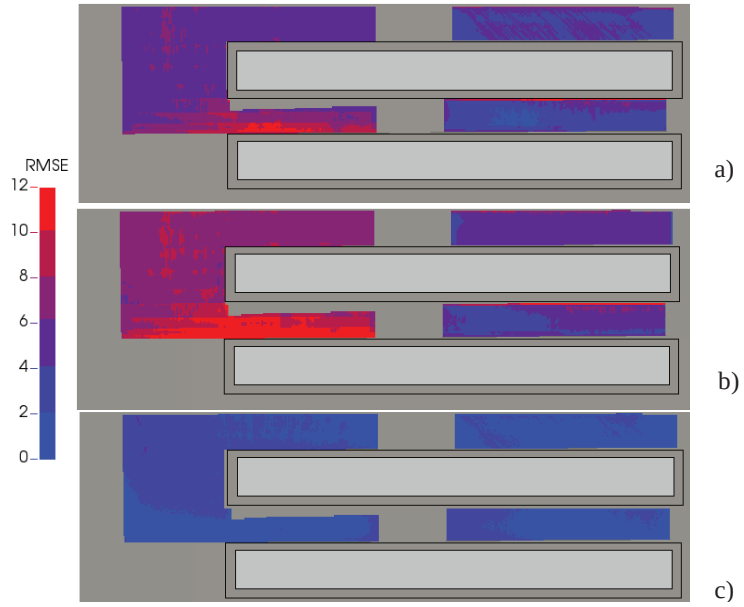

Fig. 4. RMSE of the simulations compared to the IR measurements during episode A (left) and B (right) a) whole periods b) daytimes, c) night times

temperatures, the accuracy of method is not as precise as surface temperature probes. Figure 4 shows the RMSE for the whole periods a), for the night times, b) and for the daytimes, c). Large areas of the façade has a lower RMSE than 4 degrees for the whole period. However, episode A with the higher temperatures shows larger errors than episode B with lower temperatures. The area with the highest error is where the shadows of the neighbouring building and a tree is traveling across the façade during the day. The shadow from the neighbouring building is simulated, but the timing of the shadow is slightly out of synch with the measurements something that creates a large error. In addition, the error in the area immediately below the window sill is large, probably because of the metal sheeting which is not included in the simulations. The lowest error occurs during the night when the RMSE is below 2 ^{0}C for large parts of the façade. The distribution of error shows some of the difficulties of validating a

spatial model with point data. Judging from the point values in table 1, the model seems to perform very good. However, if the aim of the simulation is to calculate accurate temperatures in time and space, Figure 4 shows that this requires extreme detail in the geometrical modelling. If however, the aim of the simulation is to calculate the climatological conditions, in which synchronization between simulation and measurements is of lower importance, the task is easier.

Figure 5 shows the measured and calculated MC for the three points on the wall for a period of approximately 10 days. In addition, the ambient RH, the rain and the wind speed at the measurement station are shown. The general trend in the moisture variation is well captured by the simulations. During the days of raining, the wind speed and direction causes driving rain to wet the area where pt3 is located. Both the measurements and the simulations capture this. Pt3 receives more driving rain than pt 1 and pt 2, something which is captured by the simulations. The measured MC should only be taken as an indication of moisture content, as these resistive measurements can have multiple sources of error, specially when mounted on the outside façade as in this case.

5. Conclusion

The paper describes a combination of models to simulate micro climate on a façade. Measured temperatures and MC in the façade suggests that the simulation of these parameters is well captured in some areas of the façade. However, the simulations show that the RMSE of the model in some parts of the façade is considerably higher than other parts. The reason for this is presumably the shadow of a nearby three and a slight time shift between measurements and simulations of the shadow of a neighboring building. This illustrates some of the difficulties in validating simulation models with full-scale outdoor measurements. A future use of the models might be the simulation of climatic deterioration of building facades for estimation of service life and decision support for architects in the use of façade material.

Acknowledgment
This work has been funded by the Norwegian Research Council in the project “WOOD/BE/BETTER” code 225345.

References

1. Hukka, A. & Viitanen, H. 1999. A mathematical model of mould growth on wooden material. *Wood Science and Technology* 33:475-485.
2. Thelandersson, S. & Isaksson, T. 2013 Mould resistance design (MRD) model for evaluation of risk for microbial growth under varying climate conditions. Building and Environment 65:18-25.

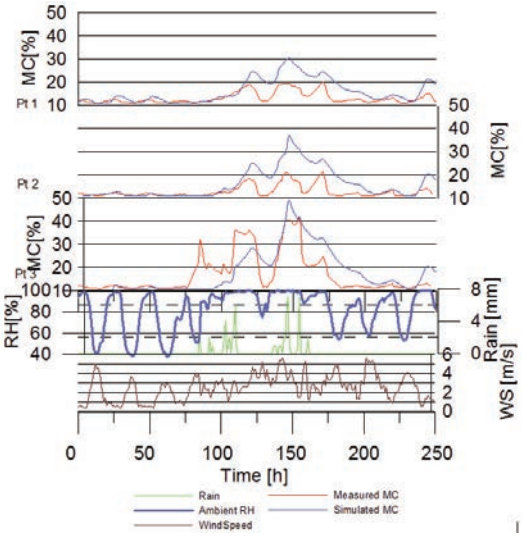

Fig. 5. Results from measurements and simulations, MC, ambient RH, wind speed and rain

3. Reinhart, C.F. & Walkenhorst, O. 2001. Validation of Dynamic RADIANCE-based Daylight Simulations for a Test Office with External Blinds. Energy and Buildings 33:683-97.
4. Bolton, D. 1980. The computation of equivalent potential temperature. Monthly Weather Review 108:1047.
5. He, X. & Lau, A.K. & Sokhansanj, S. & Lim, C.J. & Bi, X.T. & Melin, S. & Keddy, T. 2013 Moisture sorption isotherms and drying characteristics of aspen.Biomass and Bioenergy 57:161–167.
6. Mazzanti, P. & Uzielli, L. 2009. Time to reach the equilibrium moisture content: laboratory tests on Poplar (Populus alba.) mock-up panels. DISTAF, University of Florence, Italy.
7. Blocken , B. & Derome, D. & Carmeliet, J. 2013. Rainwater runoff from building facades: A review. Building and Environment 60:339–361.
8. Blocken , B. & Carmeliet, J. 2004. A review of wind-driven rain research in building science. Journal of Wind Engineering and Industrial Aerodynamics 92:1079–1130.
9. Beijer O. 1977. Concrete walls and weathering. RILEM/ASTM/CIB Symp. on Evaluation of the Performance of External Vertical Surfaces of Buildings, vol. 1, Otaniemi, Espoo,Finland, 28–31 August and 1–2 September 1977, 67–76.
10. ISO. Hygrothermal performance of buildings – Calculation and presentation of climatic data – Part 3: Calculation of a driving rain index for vertical surfaces from hourlywind and rain data. ISO 15927-3:2009 International Organization for Standardization, 2009.
11. Samuelsson, A. (1990). Resistanskurvor für elektriska fuktkvotsmätare. TräteknikCentrum, Rapport L 9006029. Stockholm. 37 pp.
12. Yang, X., Zhao, L., Bruse, M., Meng Q., (2013) Evaluation of a microclimate model for predicting the thermal behavior of different ground surfaces, Building and Environment 60:93-104
13. Chai, T., Draxler, R. R., (2014) Root mean square error (RMSE) or mean absolute error (MAE)? – Arguments against avoiding RMSE in the literature Geosci. Model Dev., 7, 1247–1250, 2014